



# The characteristic identification of disc brake squeal based on ensemble empirical mode decomposition

Yao LIANG<sup>1</sup>; Hiroshi YAMAURA<sup>2</sup>

<sup>1</sup> Tokyo Institute of Technology, Japan

<sup>2</sup> Tokyo Institute of Technology, Japan

## ABSTRACT

Disc brake squeal, which is considered as a self-excited vibration induced by friction force, has received much attention over decades due to the high customer requirements of the NVH properties of vehicles. This paper presents a characteristic identifying method for the disc brake squeal by analysing the acoustic brake squeal signal obtained from experiment. The sound of brake squeal was recorded with a sound level meter to obtain the acoustic signal that later is examined by implementing several different signal processing methods. Firstly, the Fast Fourier Transform and the Short-Time Fourier Transform are performed to illustrate the frequency components of the signal and their evolution with time. Later, the acoustic signal is analyzed using ensemble empirical mode decomposition (EEMD) which is improved from empirical mode decomposition (EMD) by adding white noises of finite amplitude to the original acoustic signal to alleviate mode mixing problem occurred in EMD. After the implementation of EEMD, the original signal is decomposed into several intrinsic mode functions (IMFs). Finally, the Hilbert Transform is conducted for revealing the detailed information about the frequency and amplitude features of each calculated IMF.

Keywords: Disc brake squeal, EEMD I-INCE Classification of Subjects Number(s): 11.8.1

## 1. INTRODUCTION

Disc brake squeal has received much attention over decades in the view of the high customer requirements of the NVH properties of vehicles, which is a complicated problem of great research value. Disc brake squeal is viewed as a self-excited vibration induced by friction force, whose frequency range is from 1KHz to 20KHz. In spite of considerable effort has been made to investigate this conundrum analytically (1), computationally and experimentally, however, still no widely accepted mechanism can explain all the brake phenomena successfully. As a result, the characteristic of the brake phenomena should be first extracted carefully to facilitate a deep understanding for later the construction of a comprehensive mechanism for brake squeal.

One way to test the characteristic of the brake squeal is to employ the finite element method (FEM) with a 3-dimensional model of the brake system and there has been extensive researches regarding the mechanisms of disc brake squeal. For example, early in 1989 Liles applied complex eigenvalue analysis to assess the stability of a finite element brake system model and parametric effects on stability were investigated for friction coefficient, pad geometry and calliper stiffness (2). Later in 2006 AbuBakar, A.R. and Ouyang, H. utilized a finite element model to predict squeal frequencies using both complex eigenvalue analysis and dynamic transient analysis with different contact regimes (3). Whereas, due to the complexity of the real brake system and the fickleness of the operational conditions (such as the humidity, the ambient temperature and the wear effects), it is difficult to include all these details into a FE model, hence the model adopted in the FEM is always a simplified model. Consequently, the characteristic of the brake squeal predicted by the simplified model without taking many details and actual operational conditions into consideration is of low reliability and confidence. The analysis based on the experimental data under real operational condition recorded from an experimental rig is considered of the ability to provide more accurate information about the signatures of brake squeal phenomena.

In this study, a characteristic identification method for disc brake squeal is introduced by analysing the recorded acoustic signal acquired from a sound level meter of the squealing brake disc and the vibration

---

<sup>1</sup>liang.y.af@m.titech.ac.jp

<sup>2</sup>yamaura@mech.titech.ac.jp

signals obtained from accelerometers mounted on the brake system of the brake components (caliper, pad and rotor) . This identification was implemented by examining the frequency-time-energy features of these acquired signals, which is based on the basic signal processing method (Fast Fourier Transformation (FFT) and Short-Time Fourier Transformation (STFT)), ensemble empirical mode decomposition (EEMD) and Hilbert transform. It is found that FFT and STFT are not sufficient to provide detailed information about the features of the fugitive squeal phenomena, and the EEMD can successfully separate the frequency components clearly. With the help of Hilbert transform, the Hilbert spectrum is computed to reveal the frequency and energy features of the squealing signals.

## 2. METHODOLOGY

In this part, firstly the experiment set-up and measurements used to acquire the acoustic signal and vibration signals are explained briefly. Lately, the signal processing methods applied to analyse the acoustic signal are introduced concretely.

### 2.1 Experiment

In this study, the acoustic signal was obtained under a practical operational condition from a validated experimental rig principally including caliper, disc, rotor, servo motor and a barometric pump. The sound pressure level of the squealing phenomenon was recorded with a sound level meter (type LA-5560 from ONO SOKKI CO.,LTD) whose measurement scale is from 20 Hz to 20 KHz and the embedded microphone (type MI-1233) has a sensitivity of 34.6 mV/Pa or -29.2 dB re. 1 V/P at 1000 Hz. The sound level meter was placed at a distance of 30 centimeters from the disc center in the disc axis direction as exhibited in Figure. 1. In addition to the sound level meter, there were three accelerometers mounted on the calliper (outside and left part of caliper), pad (outer pad, over the disc center) and rotor (at the circumference of the inside vented rotor) respectively as presented in Figure 2. The NI PX1e-1073 type national instrument was used to collect the data measured from sound level meter and accelerometers simultaneously at a sampling frequency of 44.1 KHz.

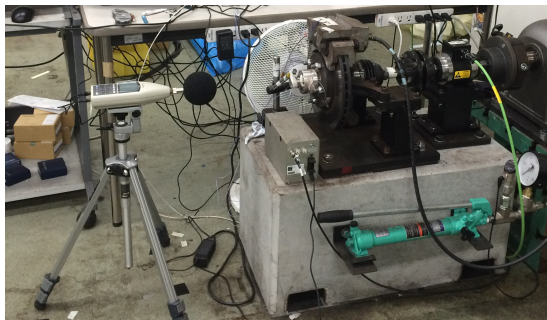


Figure 1 – The experiment setup

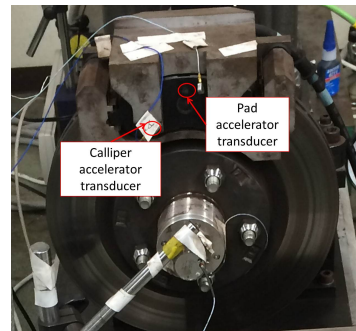


Figure 2 – The acceleration transducers

### 2.2 Fast Fourier Transform

Fourier transform considered as the most common tools for analysing periodic variances can reconstruct the original signal by taking a sum of trigonometric functions with different frequencies (4). The standard Fourier transform is denoted in Eq. (1). The Fast Fourier transform is widely applied to compute the discrete Fourier transform rapidly (5). Therefore, in this study the FFT is first applied to provide a rough idea of the frequency components in the acoustic signal. However, since the FFT is only able to decompose the stationary data (the frequency components do not change much with time), the results obtained from FFT are not reliable to reveal the intrinsic variability of non-stable squealing data. More sophisticated signal processing method should be executed later to extract the frequency features.

$$F(\omega) = \int_{-\infty}^{\infty} x(t)e^{-j\omega t} dt \quad (1)$$

### 2.3 Short-time Fourier Transform

Short-time Fourier Transform (STFT) is a Fourier-related transform which is used to determine the frequency contents of local sections over time (6). The STFT of a certain signal  $x(t)$  is given by Eq. (2), where  $w(t)$  is the window function. From this equation, it is clear to see that STFT executes: first, dividing the original signal into small portions with the implementation of window function, then performing the Fourier transform for each selected section  $x(t)w(t - \tau)$  with the increase of time giving the result  $X(\tau, \omega)$ . In each

section, the local signal can be considered as stationary, thus the regular Fourier transform can be calculated. Consequently, the STFT spectrum can plot the power density contributions for each frequency along with time, which is usually used for indicating the time-frequency-energy variation of the signals. Moreover, the length and the type of window function affect the results severely. The length determines the resolution, whereas one can not reach high frequency and time resolution at the same time. The window used influences the leakage of the signal, and only with little leakage the result obtained from STFT is of high reliability. In addition, the local signals are supposed to be time-independent with constant frequencies to give meaningful STFT results (7), nevertheless, in reality, the squealing signals are always non-stationary signals (8). Accordingly, the non-stationary signals should be tested in a more delicate method.

$$STFTx(t)(\tau, \omega) \equiv X(\tau, \omega) = \int_{-\infty}^{\infty} x(t)w(t - \tau)e^{-j\omega t} dt \quad (2)$$

## 2.4 Ensemble Empirical Mode Decomposition

On account of the insufficiency of Fourier Transform for processing the non-stationary and nonlinear data, Empirical mode decomposition method (EMD) developed by Huang et al (9) is adopted in this study to reveal the features of the fugitive squealing signals. EMD is an empirical method to adaptively and effectively separate any complicated data (especially non-stationary and nonlinear data) into a finite set of various scales naturally with a data-dependent basis. The basis consists of several signal sets with variational amplitudes and frequencies which are named as the intrinsic mode functions (IMFs). These IMFs can be used to represent the original data and they usually offer a physically meaningful representation of the original signals (10, 11). To be considered as an IMF, it has to satisfy two conditions (12):

- At any point, the mean value of the upper and lower envelope is zero,
- In the whole data set, the number of extrema and the number of zero crossing must be either equal or at most differ by one

EEMD is built on EMD by taking the mean of the IMFs obtained from EMD. Each IMF is achieved by applying EMD to the signals added by Gaussian white noise. This process utilizes the property of white noise (having an equal amount of energy on every frequency domain) to enhance the decomposition by providing a uniform reference scale distribution to avoid the mode mixing problem occurred in EMD. The procedure of this white noise-added data analysis method is (13):

- First, add a white noise with small value standard deviation (usually 0.2) to the original dataset,
- Then, the intrinsic mode functions (IMFs) of this newly formed signal are calculated based on EMD,
- Carry out this adding noise and EMD certain times,
- Later, all the obtained IMFs are averaged to get the new IMFs.

After the EEMD, the original signals can be reconstructed as Eq. (3), where  $c_i$  is the IMF and  $r_n$  is the residual.

$$x(t) = \sum_{i=1}^n c_i + r_n \quad (3)$$

## 2.5 Hilbert Transform

In this study, the Hilbert transform is implemented to finally compute the instantaneous amplitude and instantaneous frequency with physical meaning (14). Hilbert transform is used to change the time series (data) into analytical data, which is notated as Eq. (4):

$$y(t) = H[x(t)] = \frac{PV}{\pi} \int_{-\infty}^{\infty} \frac{x(\tau)}{t - \tau} d\tau, \quad (4)$$

where PV indicates the Cauchy principal value. The analytical signal  $z(t)$  is defined as the complex conjugate pair composed of  $x(t)$  and  $y(t)$  as expressed in Eq.(5)

$$z(t) = x(t) + jy(t) = A(t)e^{j\theta(t)}, \quad (5)$$

where

$$A(t) = \sqrt{x(t)^2 + y(t)^2}, \quad \text{and} \quad \theta(t) = \arctan \frac{y(t)}{x(t)} \quad (6)$$

Now the instantaneous amplitude can be obtained as  $A(t)$  and the instantaneous frequency can be simply calculated by taking first derivative of the phase function  $\theta(t)$  as:

$$\omega(t) = \frac{d\theta(t)}{dt} \quad (7)$$

Therefore, for each IMF  $c_i(t)$ , it can be written as:

$$c_i(t) = A_i(t) \cos \theta_i(t) = A_i(t) \cos \left( \int \omega_i(t) dt \right) = R(A_i e^{j\theta_i(t)}), \quad (8)$$

in which  $R$  means the real part. With this expression, the frequency-time distribution of the amplitude is designated as the Hilbert spectrum,  $H(\omega, t)$  which represents the amplitude changing features with variation of time and frequency of the analysing signals.

Consequently, the original squealing signal can be reconstructed as Eq. (9) by applying the Hilbert transform to each IMF obtained from EEMD and leaving out the residue which is either a monotonic function or a constant purpose (9).

$$x(t) = \sum_{i=1}^n A_i(t) \cos \theta_i(t) \quad (9)$$

This expansion is a generalized Fourier transform consisting of the instantaneous frequencies and instantaneous amplitudes of each IMF. This suggests that the original non-stationary and nonlinear squealing signals can be expressed as a decomposition based on a posteriori-defined basis which are the functions of time. In this sense, non-stationary and nonlinear squealing signals can be decomposed with the adaptive self based scales with meaning underlying physical meanings.

### 3. RESULTS

In this part, the original sound pressure level and the accelerations of pad, caliper and rotor of a specific squeal phenomenon are first introduced as in Figure 3. This figure depicts that the squeal lasts for almost 1.0 s and the average sound pressure level measured by the sound level meter is around 118 dB. Thus, this squeal phenomenon can be regarded as considerable noisy and annoying. The accelerations of pad and calliper experienced high level vibrations during the squealing period, on the other hand, the acceleration of rotor is relatively low almost near 0 m/s<sup>2</sup>.

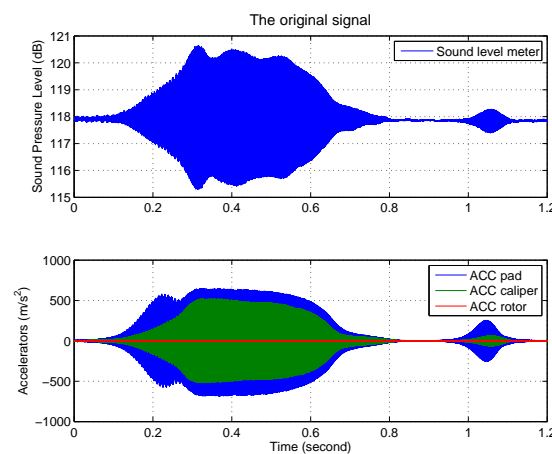


Figure 3 – The original signals obtained from sound level meter and accelerometers

Subsequently, the results of the Fast-Fourier transformation, Short-Time Fourier transformation are explained, which offer a brief understanding of the specific squealing phenomenon's frequency components and also the energy-frequency revolution with the variation of time. Furthermore, the EEMD result of this squealing signal is depicted and interpreted, which explicates only the first two IMFs are the dominate components with rather high amplitudes which can be used to reconstruct the original squealing signal.

#### 3.1 FFT and STFT results

The FFT results of the specific squealing signal and also the simultaneous vibration signals of caliper, pad and rotor are provided in Figure 4. This figure exhibits that the dominant frequency component for sound level meter is 7.6 KHz. Frequency components under 2 KHz with relatively low amplitude are regarded as mechanical background noises. Apart from these, at 11.38 KHz and 15.2 KHz, there are also two minor peaks with considerable low amplitude which have the possibility of developing into the primary frequency components. Consequently, the squeal's main frequency should be considered as 7.6 KHz. Similarly, from the FFT results of pad and caliper, the frequency component 7.6 KHz also has high amplitude and frequency

components 11.38 KHz and 15.2 KHz have low amplitude. while the FFT result of rotor illustrates that it has frequency components 5 KHz , 9 KHz and 18 KHz , at where the sound level meter, accelerations of caliper and rotor don't have, with comparatively low amplitude which is which is only one-hundredth of the ones of caliper and pad.

The result of STFT pictured in Figure 5 elucidates that the squealing signal primarily consists of 7.58 KHz and 11.37 KHz frequency components and it has background noises in the low frequency domain. The STFT results of the sound level meter verify that the squeal is not stable and it varies quite a lot with time. Similar results can be observed in the STFT consequences of accelerations of caliper and pad, nonetheless, in addition to the frequency components around 7.5 KHz and 11KHz another frequency components 15.5 KHz and 19.47 KHz appear. Besides, for the rotor, the STFT result demonstrates that it has three frequency components (5 KHz, 9.3 KHz, 18.43 KHz) with relatively low energy.

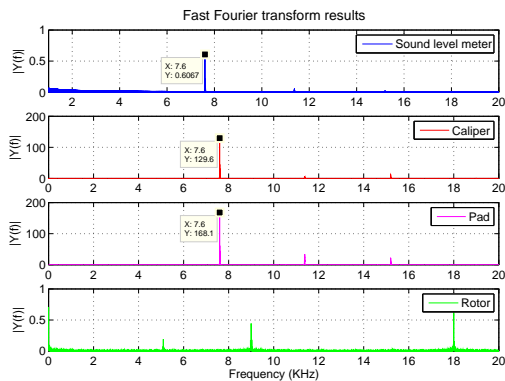


Figure 4 – The FFT results

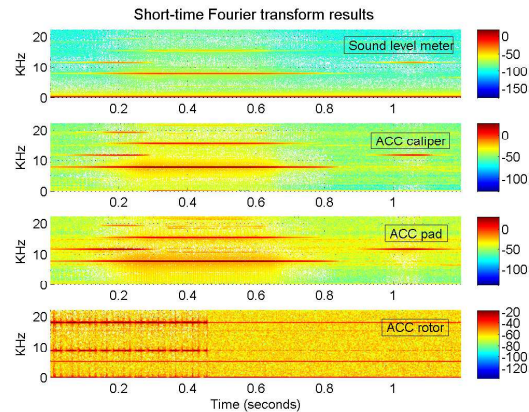


Figure 5 – The STFT results

### 3.2 EEMD results

The EEMD algorithm was executed with 100 iterations of the EMD algorithm with adding Gaussian white noise to the original signals and added Gaussian white noise's standard deviation is 0.2 which is recommended in literature (13). The resultant Figure 6 displays the EEMD result of the squeal signal (the signal measured by sound level meter), it reveals that for the brake squeal signal the first 2 IMFs with considerable high amplitudes are considered as the main explanations for the squeal phenomenon. Moreover, among the first two IMFs, the first IMF is the dominant one with 5 times amplitude of the second IMF. Since EEMD computes the IMFs from the highest frequency to the lowest one, the first 2 IMFs have higher frequencies than the other IMFs.

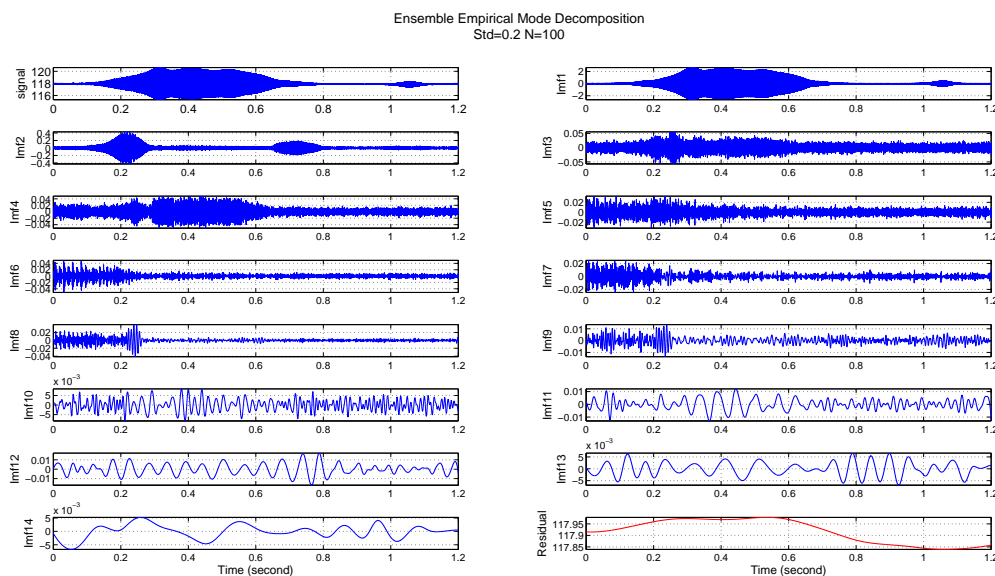


Figure 6 – The EEMD result for brake squeal

In order to examine the IMFs in details to survey the frequencies of the IMFs, the Hilbert transform was conducted and the instantaneous amplitudes and instantaneous frequencies for the first 3 IMFs are plotted in Figure 7, in which the third row for the third IMF is portrayed as a comparison to the first and second IMFs. This figure reveals that the first IMF started from 0.4 s and lasted to 0.7 s with relative high amplitude and has a little protuberance at 1 s and that lasted for 0.1 s. The instantaneous frequency of the first IMF is around 7.5 KHz from 0.3 s to 0.6 s and around 11.5 KHz lasted for only 0.1 s from 1 s. This again demonstrates that the squeal signal is non-stationary signal. The Hilbert spectrum in the third column indicates that the main frequency is around 7.4 KHz with comparatively high energy. In addition, the frequency around 11.4 KHz appears at 0.16 s and 1.06 s. This illustrates that the high frequency component appears firstly with lower energy and later the low frequency component arises with a higher level of energy which leading the squeal to develop into the mature stage. For the second IMF, the main frequency is around 7.6 KHz. The third IMF's instantaneous frequency is mainly around 5.5 KHz but of high energy at 7.6 KHz. The instantaneous amplitude and instantaneous frequency of third IMF is depicted for contrast. It is evident that the instantaneous amplitude is fairly low and the instantaneous frequency is almost uniformly contributed due to the added Gaussian white noise. Consequently, the squeal is regarded chiefly constructed of 7.5 KHz and also has 11.5 KHz components, which is in accord with the results of FFT and STFT, but offers more detail information about the variance of the signal.

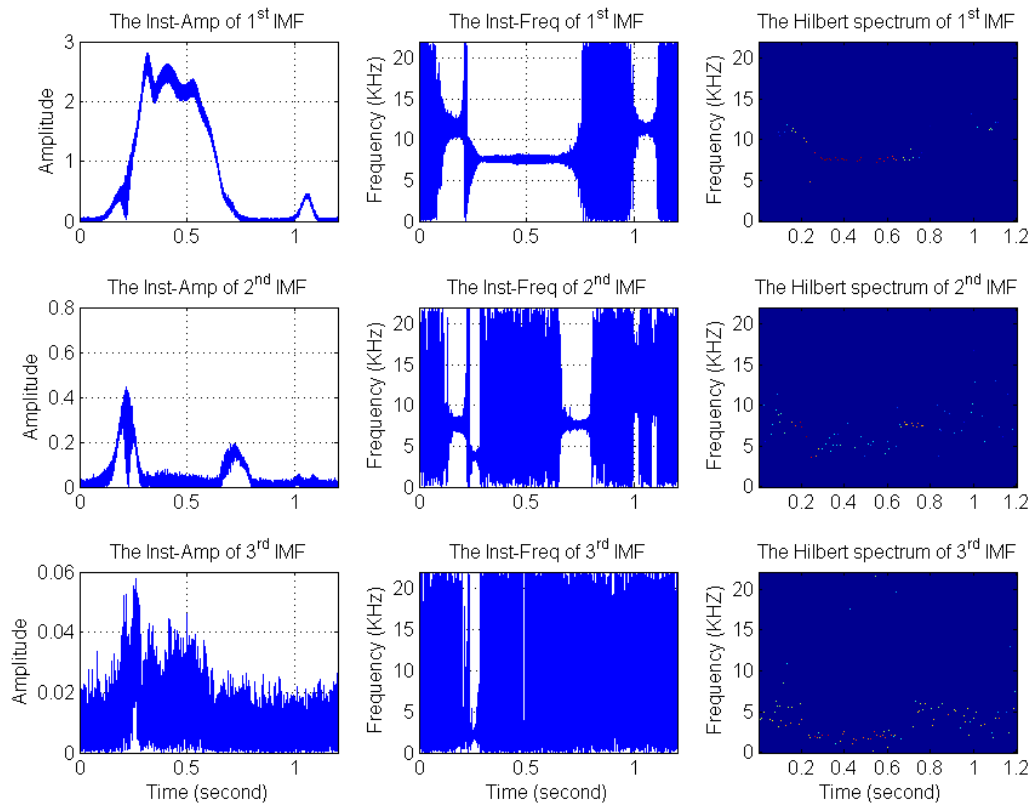


Figure 7 – The Inst-amp, inst-frequency, Hilbert spectrum for first 3 IMFs of squeal signal

In an analogous manner, the EEMD was implemented for acceleration signals of caliper, pad and rotor and the results are presented in Figure 8, Figure 9 and Figure 10 respectively. The behaviours of the instantaneous amplitudes and instantaneous frequencies of caliper and pad's accelerations are quite similar to the ones of squeal signal. By contrast, the behaviours of the rotor's vibration signal are quite different. The IMFs of rotor's vibration signal only has substantial instantaneous amplitude before 0.4 s and the instantaneous frequency for the first IMF is around 18.5 KHz, 9 KHz and 5 KHz for the second and third IMFs respectively. Frequency components after 0.4 s are caused by the added Gaussian white noise. These results again in accord with the results of FFT and STFT, but provide more detailed information about the changes of the signals.

#### 4. CONCLUSIONS

From the results discussed earlier, the conclusion can be drawn that the 7.6 KHz is the main frequency component of the squeal signal with high energy and lasts longer and it was caused by the resonance of caliper and pad who have the same frequency component. Additionally, the 11.5 KHz is also the frequency component but with comparatively low energy and last for only a short period which is also caused by the resonance of caliper and pad but with lower energy. In this particular squeal phenomenon, the high frequency component displays in the beginning and laterly the low frequency component shows up with high amplitude. As a consequence, it is considered that the higher frequency resonance can induce the lower frequency resonance which makes the squeal phenomenon evolve into its mature stage. In addition, the high frequency component may take over the predominance when the amplitude grows larger than the one of 7.6 KHz. For the rotor, since the amplitude of the vibration is considerably lower and with different frequency component of squeal signal, therefore, it is not the source of the squealing phenomenon.

The EEMD method adopted in this study can provide more information on the non-stationary squeal signal such as the instantaneous amplitude and instantaneous frequency, nevertheless, it still has the mode mixing problem when decompose the squeal signal and the acceleration signals of caliper and pad. The may be caused by the inappropriate amplitude of Gaussian white noise. The next study should be focused on this problem.

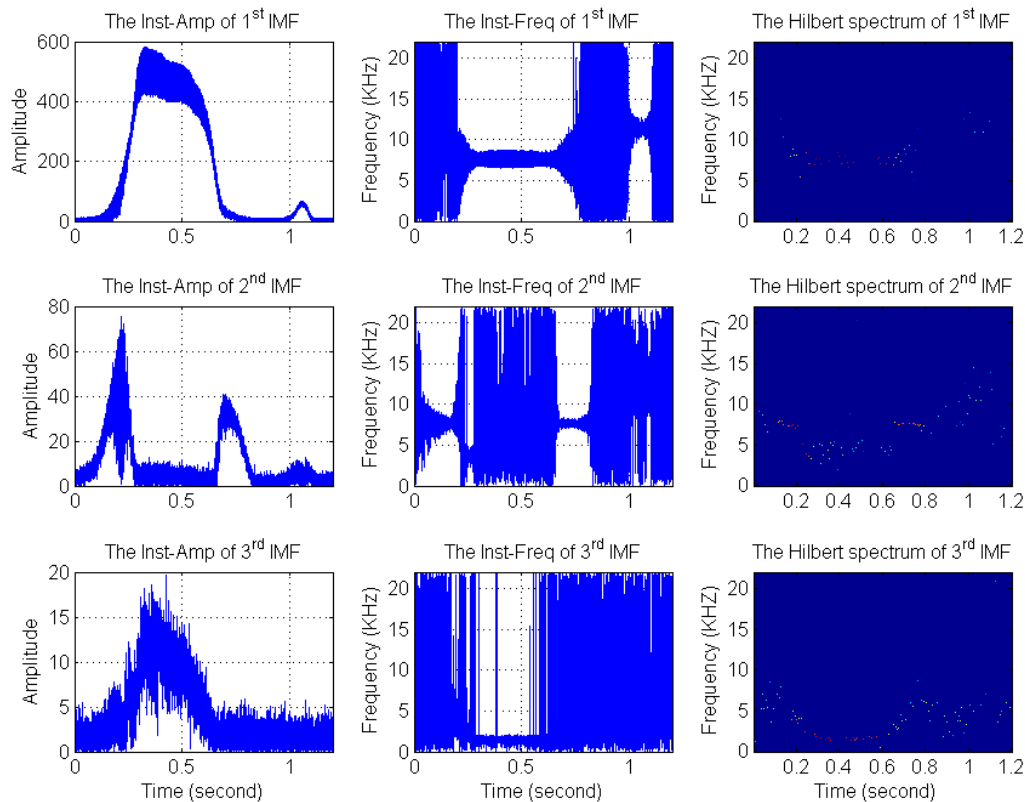


Figure 8 – The Inst-amp, inst-frequency, Hilbert spectrum for first 3 IMFs of caliper vibration signal

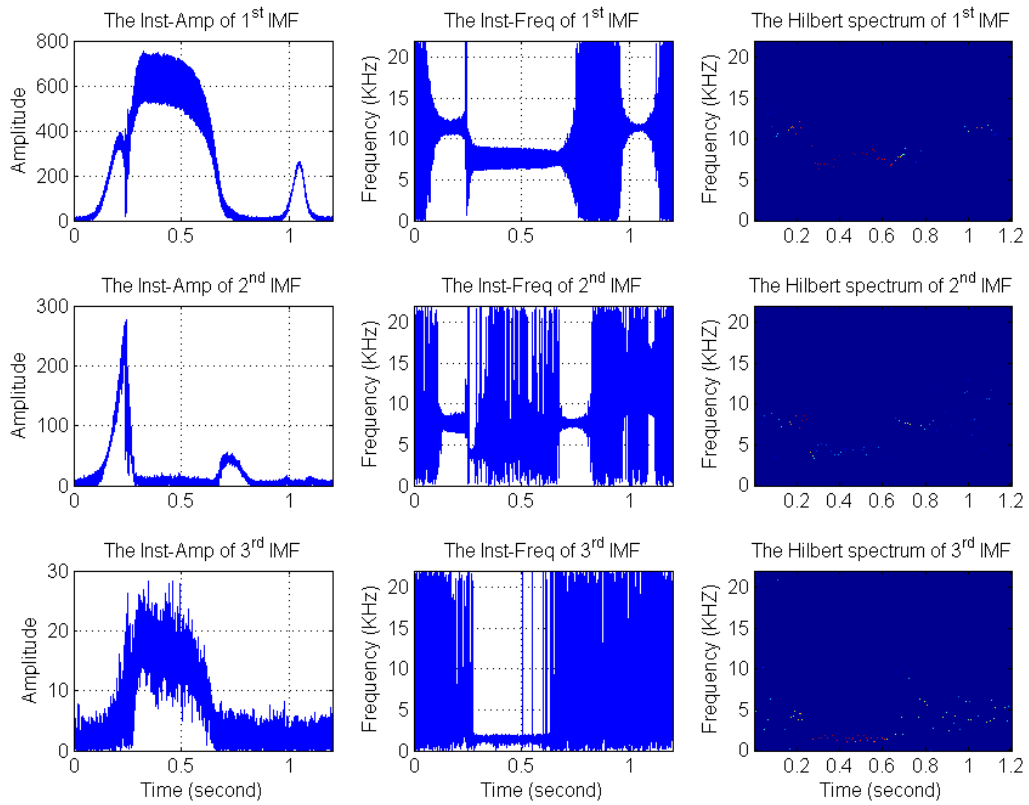


Figure 9 – The Inst-amp, inst-frequency, Hilbert spectrum for first 3 IMFs of pad vibration signal

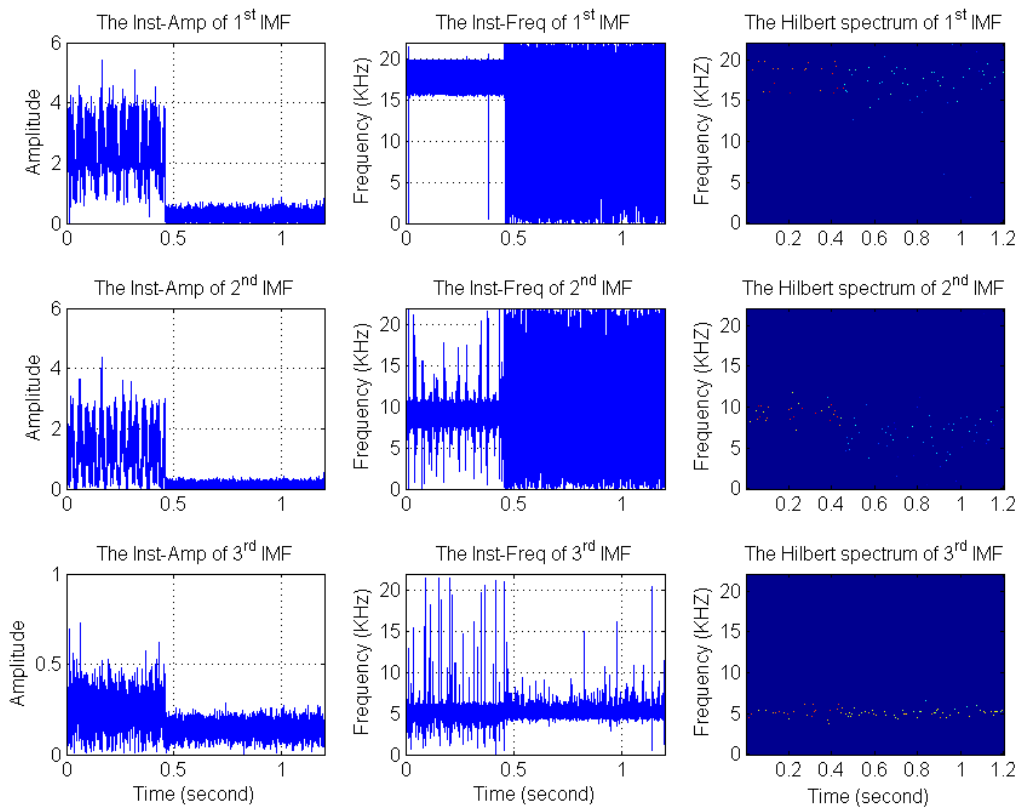


Figure 10 – The Inst-amp, inst-frequency, Hilbert spectrum for first 3 IMFs of rotor vibration signal



## REFERENCES

1. Kinkaid N, O'Reilly O, Papadopoulos P. Automotive disc brake squeal. *Journal of sound and vibration*. 2003;267(1):105–166.
2. Liles GD. Analysis of disc brake squeal using finite element methods. SAE Technical Paper 891150; 1989.
3. AbuBakar AR, Ouyang H. Complex eigenvalue analysis and dynamic transient analysis in predicting disc brake squeal. *International Journal of Vehicle Noise and Vibration*. 2006;2(2):143–155.
4. Bracewell RN, Bracewell R. *The Fourier transform and its applications*. vol. 31999. McGraw-Hill New York; 1986.
5. Van Loan C. *Computational frameworks for the fast Fourier transform*. vol. 10. Siam; 1992.
6. Cohen L. *Time-frequency analysis*. vol. 778. Prentice Hall PTR Englewood Cliffs, NJ.; 1995.
7. Qian S. *Introduction to time-frequency and wavelet transforms*. Prentice Hall; 2002.
8. Yang F, Tan CA, Chen F. Application of the Empirical Mode Decomposition Method to the Identification of Disc Brake Squeal. In: *ASME 2002 International Mechanical Engineering Congress and Exposition*. American Society of Mechanical Engineers; 2002. p. 777–783.
9. Huang NE, Shen Z, Long SR, Wu MC, Shih HH, Zheng Q, et al. The empirical mode decomposition and the Hilbert spectrum for nonlinear and non-stationary time series analysis. *Proceedings of the Royal Society of London Series A: Mathematical, Physical and Engineering Sciences*. 1998;454(1971):903–995.
10. Wu Z, Huang NE. A study of the characteristics of white noise using the empirical mode decomposition method. *Proceedings of the Royal Society of London Series A: Mathematical, Physical and Engineering Sciences*. 2004;460(2046):1597–1611.
11. Rilling G, Flandrin P, Goncalves P, et al. On empirical mode decomposition and its algorithms. In: *IEEE-EURASIP workshop on nonlinear signal and image processing*. vol. 3. NSIP-03, Grado (I); 2003. p. 8–11.
12. Torres ME, Colominas MA, Schlotthauer G, Flandrin P. A complete ensemble empirical mode decomposition with adaptive noise. In: *Acoustics, Speech and Signal Processing (ICASSP), 2011 IEEE International Conference on*. IEEE; 2011. p. 4144–4147.
13. Wu Z, Huang NE. Ensemble empirical mode decomposition: a noise-assisted data analysis method. *Advances in adaptive data analysis*. 2009;1(01):1–41.
14. Huang NE, Shen SS. *Hilbert-Huang transform and its applications*. vol. 5. World Scientific; 2005.